The Plant Cell, Vol. 22: 34–47, January 2010, www.plantcell.org © 2010 American Society of Plant Biologists

Cooperation of Multiple Chromatin Modifications Can Generate Unanticipated Stability of Epigenetic States in *Arabidopsis* [C][W][OA]

Tuncay Baubec,[a,1] Huy Q. Dinh,[a,b] Ales Pecinka,[a] Branislava Rakic,[a] Wilfried Rozhon,[a,2] Bonnie Wohlrab,[a] Arndt von Haeseler,[b] and Ortrun Mittelsten Scheid[a,3]

[a] Gregor Mendel Institute of Molecular Plant Biology, Austrian Academy of Sciences, 1030 Vienna, Austria
[b] Center for Integrative Bioinformatics Vienna, Max F. Perutz Laboratories, University of Vienna, 1030 Vienna, Austria

Epigenetic changes of gene expression can potentially be reversed by developmental programs, genetic manipulation, or pharmacological interference. However, a case of transcriptional gene silencing, originally observed in tetraploid *Arabidopsis thaliana* plants, created an epiallele resistant to many mutations or inhibitor treatments that activate many other suppressed genes. This raised the question about the molecular basis of this extreme stability. A combination of forward and reverse genetics and drug application provides evidence for an epigenetic double lock that is only alleviated upon the simultaneous removal of both DNA methylation and histone methylation. Therefore, the cooperation of multiple chromatin modifications can generate unanticipated stability of epigenetic states and contributes to heritable diversity of gene expression patterns.

INTRODUCTION

Genetically determined loss of gene expression by mutation, insertion of transposons, or chromosomal rearrangements is usually irreversible, since the chance of precisely reconstituting the original DNA sequence is low. On the other hand, epigenetic loss of gene activity is defined as not affecting the DNA sequence but rather as chemically modifying DNA and associated proteins, thus altering the packaging of chromatin and its accessibility for the transcription machinery. Affected sequences are kept transcriptionally inactive by well-characterized pathways that establish DNA methylation and/or histone modifications. For several of these modifications, antagonistic enzymes have been described (Chen and Tian, 2007; Pfluger and Wagner, 2007; Ooi and Bestor, 2008), and many epigenetically regulated sequences undergo a cycle of silencing and activation in the life cycle of the organism. Familiar examples in developmental programs are imprinted genes, dosage-compensated chromosomes, or master regulatory genes under the control of the Polycomb/Trithorax system. Even genetic templates that can produce potentially deleterious transcripts and are usually under tight epigenetic control can become activated under stress conditions (for review, see Madlung and Comai, 2004; Chinnusamy and Zhu, 2009) or in the germ line in order to reinforce silencing via small RNA during transmission of genetic material to the next generation (Brennecke et al., 2008; Slotkin et al., 2009). However, some cases of genes with very durable epigenetic marks are also known (Chong and Whitelaw, 2004), and the stable transmission of their epigenetic state to subsequent generations has led to their denotation as epialleles (Finnegan, 2002). Examples in plants are a methylated transcription factor gene changing flower morphology in *Linaria* (Cubas et al., 1999) and the pigmentation-controlling transcription factor genes in maize (*Zea mays*) that are downregulated by paramutation (for review, see Chandler et al., 2000). These famous cases were identified because of the striking phenotypes. It is likely that many more epialleles exist with less drastic morphological consequences but which nevertheless make a significant contribution to natural evolution and plant breeding (Kalisz and Purugganan, 2004).

Epialleles with remarkable stability have been observed in various tetraploid lines of *Arabidopsis thaliana* derived from a common diploid progenitor (Mittelsten Scheid et al., 2003). The transgenic resistance marker gene, hygromycin phosphotransferase (*HPT*), under the control of the strong, constitutively active promoter of the *Cauliflower mosaic virus* (P35S) was present in these genetically identical lines either in fully active or completely silenced state. Both states were maintained during backcrosses to diploid lines homozygous for the *HPT*, giving rise to diploid lines C2R (resistant to hygromycin, active *HPT*) and C2S1 (diploid, sensitive to hygromycin, silent *HPT*). In crossing experiments with the tetraploid lines, the epialleles exerted a paramutation-like interaction in which the silent epiallele led to inactivation of the previously active counterpart (Mittelsten

[1] Current address: Friedrich Miescher Institute of Biomedical Research, Maulbeerstrasse 66, CH-4058, Basel, Switzerland.
[2] Current address: Max F. Perutz Laboratories, University of Vienna, Dr. Bohr-Gasse 9, 1030, Vienna, Austria.
[3] Address correspondence to ortrun.mittelsten_scheid@gmi.oeaw.ac.at. The author responsible for distribution of materials integral to the findings presented in this article in accordance with the policy described in the Instructions for Authors (www.plantcell.org) is: Ortrun Mittelsten Scheid (ortrun.mittelsten_scheid@oeaw.ac.at).
[C]Some figures in this article are displayed in color online but in black and white in the print edition.
[W]Online version contains Web-only data.
[OA]Open Access articles can be viewed online without a subscription.
www.plantcell.org/cgi/doi/10.1105/tpc.109.072819

Scheid et al., 2003). The epialleles differ in the degree of DNA methylation and histone modification patterns (Hetzl et al., 2007; Foerster, 2009), as do many other active and inactive sequences. The epialleles show an extremely tight silencing (as described in the following): they were originally found in the tetraploid lines, and the epiallelic interaction occurred only in tetraploid intercrosses. Therefore, we refer to this phenomenon as polyploidy-associated transcriptional gene silencing (paTGS) even in the diploid lines. Most higher plants are polyploid (Masterson, 1994), and polyploidy is assumed to be a very important driving force in plant evolution and breeding (Stebbins, 1966). Furthermore, epigenetic changes are frequent in freshly formed polyploids (for review, see Osborn et al., 2003; Adams and Wendel, 2005). Paramutation-like epiallelic interaction can lead to significant shifts in the distribution of traits within populations of polyploid plants and drive their evolution more rapidly than anticipated by classical Mendelian genetics. Therefore, it is important to understand the characteristics of the epialleles that underwent paTGS. The described silent *HPT* epiallele offered an excellent model for this analysis, since its stability also in the diploid derivative line and the encoded protein allowed a selection-based genetic screen for *trans*- and *cis*-acting factors involved in the maintenance of the silencing. Here, we demonstrate that the silent epiallele derived from the tetraploid line is under a double safeguard mechanism, which requires the concomitant loss of methylation of both DNA and histones for restoration of transcription. This is in contrast with many other transcriptionally silent sequences in the *Arabidopsis* genome that can be activated by removing only one of several inactive chromatin marks by mutation or specific inhibitors. Thus, epialleles in polyploid plants cannot easily revert and represent particularly stable states that are under tight control. For this reason, they might be highly relevant for long-term adaptation of gene expression patterns, breeding, and natural evolution.

RESULTS

paTGS Is Resistant to Treatments with DNA Methylation and Histone Deacetylase Inhibitors

Transcriptional inactivation in plants and mammals is frequently associated with methylation of cytosine residues in the DNA, an exchange of specific methylation of histone tails from active to inactive marks, and general deacetylation of histone tails (Chen and Tian, 2007; Vaillant and Paszkowski, 2007). Inhibitors specific for DNA methyltransferases and histone deacetylases exist, and they have been widely used as potentially activating agents for epigenetically silenced endogenes and transgenes (Chang and Pikaard, 2005). The DNA methylation inhibitor zebularine (ZEB) (Zhou et al., 2002) and the histone deacetylase inhibitor trichostatin A (TSA) (Yoshida et al., 1995) were therefore applied to test whether they would reactivate the silent *HPT* transgene. Seeds from the diploid line C2S1 with the inactive *HPT* and seeds from the *HPT*-expressing, hygromycin-resistant line C2R were germinated and plantlets grown for 3 weeks on plates containing 10 μg/mL of hygromycin in combination with 40 μM ZEB and/or 1.6 μM TSA, concentrations that were previously described to be effective in reactivating silenced targets and reducing methylation in all possible sequence contexts (Baubec et al., 2009) or were even higher than effective concentrations (Chang and Pikaard, 2005). ZEB causes growth retardation but allows the *HPT*-expressing line C2R to grow under selection upon all treatments. By contrast, no growth was observed in line C2S1 (Figure 1A), even upon sequential application of the drugs prior to selection. The applied drug treatments could not, therefore, reactivate the HPT gene and restore the resistant phenotype.

Stringent hygromycin selection requires a certain amount of *HPT* RNA and protein to be produced. To determine whether the inhibitors would release subthreshold levels of gene expression, we performed RNA gel blot analysis using *HPT*-specific probes on total RNA extracted from C2S1 seedlings treated with 0, 20, 40, and 80 μM ZEB. These showed a minimal increase in *HPT* transcript but substantially less hybridization signal than in C2R (Figure 1B). In addition, known epigenetic mutations, such as *cmt3*, *drm1,2*, and *kyp* that could not restore hygromycin resistance after introgression of the silent C2S1 epiallele (Milos, 2006), did also not further enhance the effect of zebularine treatments (see Supplemental Figure 1 online). Surprisingly, RNA gel blot analysis with a probe for a noncoding RNA transcribed from another copy of the P35S promoter, downstream of and in close proximity to the *HPT* gene (see Supplemental Figure 2 online), revealed strong reactivation of this second transcript after ZEB treatment of C2S1 (Figure 1B). The pharmacological demethylation was effective, as demonstrated by methylation-sensitive restriction digest and subsequent DNA gel blotting (Figure 1C), but was not sufficient to reactivate the *HPT*-driving promoter.

paTGS Can Be Released by Novel *DDM1* and *HOG1* Mutant Alleles

Since the silent *HPT* transgene allowed for a reactivation assay based on hygromycin selection, we performed a forward genetic screen to identify factors involved in this robust epigenetic regulation of the *HPT* promoter. Diploid C2S1 plants carrying the silent *HPT* transgenic locus were mutagenized by random T-DNA insertion, and M2 progeny of 20,000 independent transformants was screened for hygromycin resistance. We identified three novel alleles of *DECREASE IN DNA METHYLATION1* (*DDM1*), a member of the ATP-dependent SWI2/SNF2 chromatin remodeling gene family (Vongs et al., 1993; Mittelsten Scheid et al., 1998; Jeddeloh et al., 1999) and one novel allele of the *HOMOLOGOUS GENE SILENCING1* (*HOG1*) gene, coding for an *S*-adenosyl-L-homocysteine (SAH) hydrolase (SAHH) (Furner et al., 1998; Rocha et al., 2005). Mutations in *DDM1* (At5g66750) have been previously shown to interfere with maintenance of transcriptional gene silencing at numerous endogenous and transgenic inserts by decreasing DNA and H3K9 methylation (Mittelsten Scheid et al., 1998; Jeddeloh et al., 1999; Soppe et al., 2002; Mathieu et al., 2003). HOG1 (or SAHH1, At4g13940) is required to convert SAH into homocysteine. This degradation is essential for recycling of the methyl-group donor *S*-adenosyl-L-methionine (SAM) and prevents inhibition of *trans*-methylation reactions through increased levels of SAH (Weretilnyk et al., 2001). HOG1 is involved in maintaining transcriptional gene silencing at numerous targets (Furner et al., 1998;

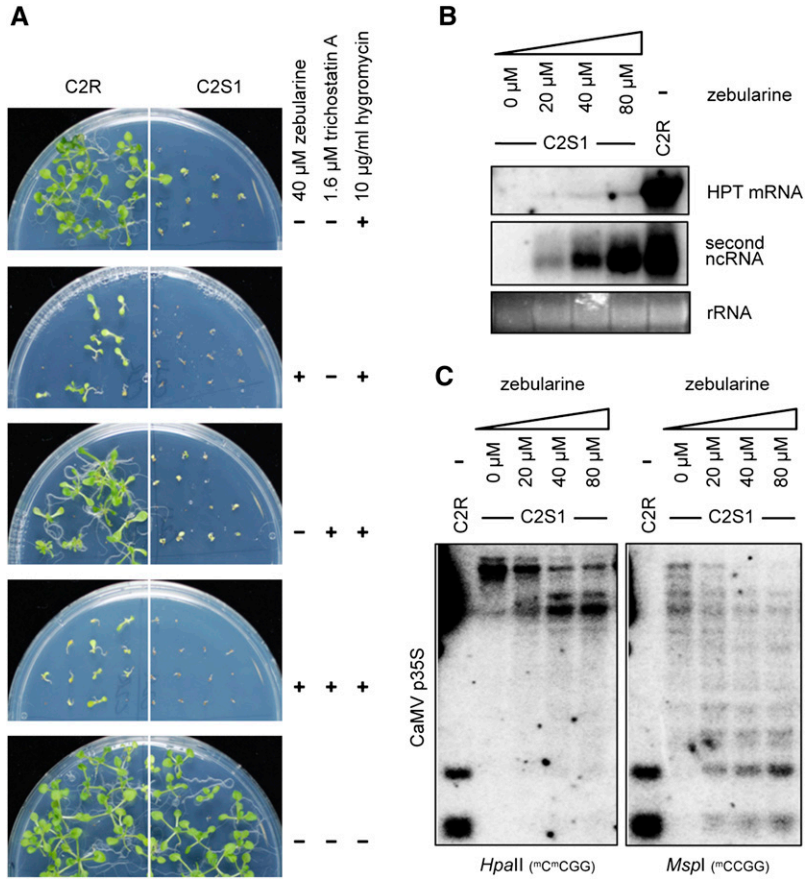

Figure 1. Treatments with DNA Methylation and Histone Deacetylase Inhibitors Do Not Release paTGS Silencing.

(A) C2R and C2S1 seedlings grown on 10 μg/mL hygromycin plates in the presence of 40 μM ZEB and/or 1.6 μM TSA.
(B) RNA gel blot analysis indicates reactivation of the second noncoding transcript but not *HPT* mRNA after 20, 40, and 80 μM ZEB treatments.
(C) DNA gel blot analysis of DNA methylation after treatments with increasing zebularine concentrations using promoter-specific probes.
[See online article for color version of this figure.]

Rocha et al., 2005; Mull et al., 2006; Jordan et al., 2007), while another SAHH-related gene (*SAHH2*, At3g23810) has no role in silencing or DNA methylation (Rocha et al., 2005). The *DDM1* alleles were named *ddm1-11* to *ddm1-13*, in continuation of the already available mutant alleles (Jeddeloh et al., 1999; Jordan et al., 2007): *ddm1-11* has a 38-bp deletion in exon V, *ddm1-12* has a 30-bp deletion in exon XIV, and *ddm1-13* has a T-DNA insertion in exon VII (Figure 2A). In contrast with the widely used alleles *ddm1-2*, with a point mutation generating a G-to-A transition in the splice donor site of intron XI (Jeddeloh et al., 1999), and *ddm1-5*, with an 82-bp insert in exon II (Mittelsten Scheid et al., 1998; Jeddeloh et al., 1999), the new mutations are all in conserved signature motifs that are characteristic of SWI2/SNF2 family proteins (Bork and Koonin, 1993) and affect the domains that are important for ATP-dependent chromatin remodeling, namely, SNF2_N and DEAD/DEAH (Figure 2A). This may explain why plants with the new alleles survived the stringent hygromycin selection in the M2 generation during the screen, while plants with the *ddm1-5* allele showed partial reactivation and survived only in F4 after introgression (Mittelsten Scheid et al., 2003; Milos, 2006). A direct comparison of the *ddm1-5* F4 seedlings with the corresponding M4 generation seedlings obtained from the novel alleles further illustrates the differences in resistance (Figure 2B), confirmed by *HPT* expression analysis (see below). *ddm1-12* was used as a representative *ddm*1 allele in the following experiments. The new *HOG*1 allele, named *hog1-7* in continuation of previously identified alleles (Rocha et al., 2005), has a rearranged T-DNA insertion in the 3′ UTR (Figure 2C). Although this mutation is not likely to cause a complete loss of function, it affects *HOG1* mRNA levels and stability, as revealed by quantitative RT-PCR (Figure 2D).

We analyzed the degree of *HPT* reactivation in 3-week-old M4 mutant seedlings. Quantification of *HPT* transcripts with real-time PCR using cDNA obtained from reverse-transcribed total RNA from the *ddm1-12* and *hog1-7* mutants indicated a similar abundance as in the active line C2R (1-fold ± 0.35 and 0.96-fold ± 0.23 in *hog1-7* and *ddm1-12* mutants, respectively; Figure 3A).

This is in agreement with a similar loss of DNA methylation at the P35S promoter, as shown by DNA gel blot analysis (Figure 3B). To quantify the degree of DNA demethylation specifically at the promoter upstream of *HPT*, we applied bisulfite sequencing

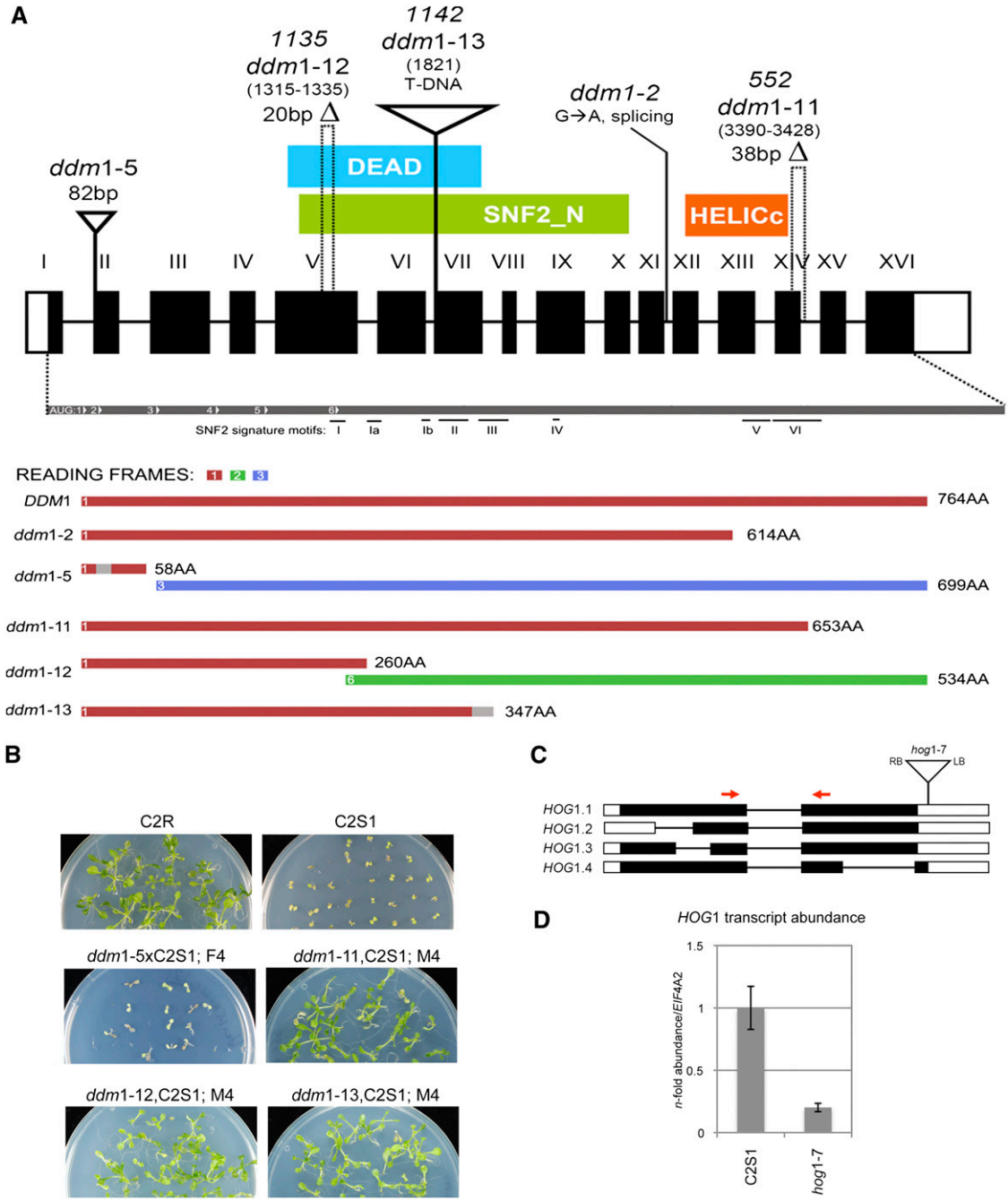

Figure 2. Novel *ddm1* and *hog1* Mutant Alleles.

(A) *DDM1* gene region with indicated UTRs (white boxes), exons (filled boxes), and introns (lines). Functional domains are indicated by colored boxes, while mutations are indicated by insertions or deletions (Δ). Below: reading frame analysis in the *ddm1* alleles. Coding sequence is indicated by the gray bar, and conserved SWI2/SNF2 signatures (Bork and Koonin, 1993) are shown below. White glyphs indicate potential translation initiation sites in the 5′ region (aa(A/G)(A/C)a**AUG**Ccg; Rangan et al., 2008). Coding reading frames (in different colors) and encoded protein size are predicted in wild-type and mutant alleles. Light-gray bars indicate nonplant DNA insertions.
(B) Allele comparison by hygromycin selection in analogous generations: F4 from crosses between C2S1 × *ddm1-5* and M4 in the novel alleles. C2S1 and C2R are used as controls.
(C) Mutant integration site in the *SAHH*/*HOG1* gene. UTRs are indicated as white boxes, exons as filled boxes, and introns as lines. The four predicted splice variants are displayed (TAIR7).
(D) Quantification of *HOG* transcript abundance in wild-type C2S1 and *hog1-7* mutant plants normalized to *EIF4A2*. Error bars represent SD from triplicate analyses. Used primers are indicated by red arrows in **(C)**.

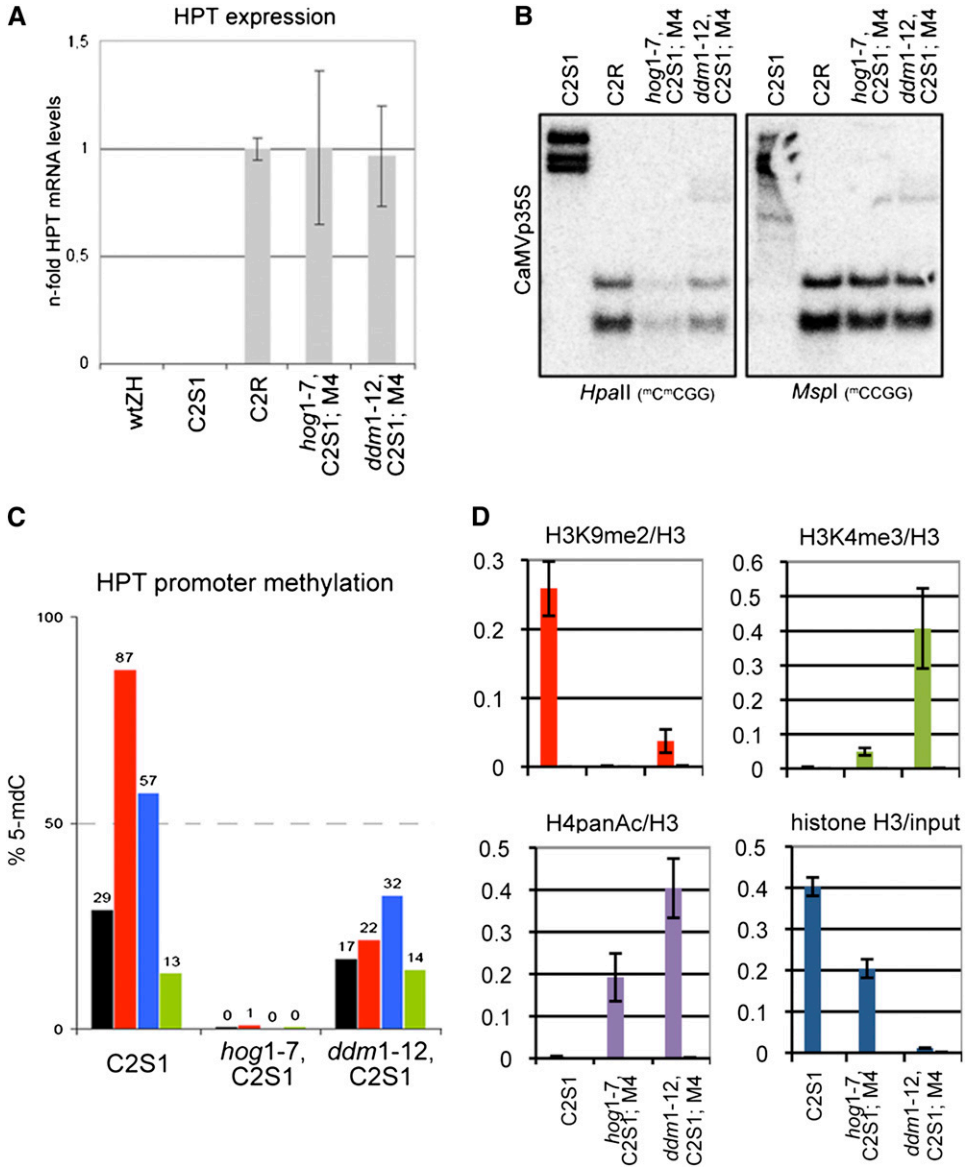

Figure 3. Mutations in *DDM1* and *HOG1* Release paTGS from the HPT Transgene.

(A) Quantification of HPT mRNA levels in wild-type, C2S1, C2R *hog1-7*,C2S1, and *ddm1-12*,C2S1 seedlings normalized to *EIF4A2*. Error bars represent SD from triplicate analyses.

(B) p35S DNA methylation analysis in C2S1, C2R, and mutant plants by DNA gel blotting of DNA digested by methylation-sensitive restriction enzymes.

(C) Promoter DNA methylation analysis by bisulfite sequencing representing total (black) and sequence context-specific (^{m}CG, red; ^{m}CHG, blue; ^{m}CHH, green) methylation.

(D) Analysis of histone modifications and histone H3 abundance normalized to H3 or input at the *HPT* promoter by ChIP in C2S1 and mutant lines. Gray columns (right of the colored columns and very small) represent samples precipitated without antibodies.

to DNA of the *hog1-7* and *ddm1-12* mutants (Figure 3C). Total DNA methylation was reduced from 29% in C2S1 to 0% in *hog1-7* and to 17% in *ddm1-12*, while CG-specific methylation was reduced from 87 to 1% and 22% in *hog1-7* and *ddm1-12*, respectively. We observed a similar decrease in methylation at CHG sites, where the *hog1-7* mutation resulted in 0% residual methylated CHG sites, while the *ddm1-12* mutation maintained 32% of the methylated CHG sites compared with 57% in C2S1. CHH-specific methylation, with 13% of all available sites in C2S1, was significantly decreased in *hog1-7* with 0%, while it remained unaltered in the *ddm1-12* mutant, indicating that DDM1 is not required to maintain methylation at these largely nonsymmetrical sites (Figure 3C).

To complement the analysis of chromatin changes in the mutants, we further analyzed *ddm1-12*–specific and *hog1-7*–specific changes in histone modifications at the *HPT* transgene promoter

by chromatin immunoprecipitation (ChIP) using specific antibodies or antisera against the heterochromatic mark histone H3 Lys-9 dimethylation (H3K9me2) and the euchromatic marks histone H3 Lys-4 trimethylation (H3K4me3) and histone H4 panacetylation (H4panAc) (for review, see Fuchs et al., 2006). General nucleosome occupancy in the examined regions was analyzed by ChIP with antibodies recognizing histone H3 independent of modifications. Enrichment of the DNA fragments in the modification-specific precipitates was measured by quantitative PCR in triplicate and was related to their loading with histone H3. The prevalence of heterochromatic H3K9me2 in C2S1 was drastically reduced in the *hog1-7* and *ddm1-12* mutants (Figure 3D, red columns). H3K4me3 increased in both mutants compared with C2S1, although only slightly in *hog1-7* and much more pronounced in *ddm1-12* (Figure 3D, green columns). An increase of H4 acetylation was observed in both mutants, again with a stronger increase in *ddm1-12* (Figure 3D, violet columns). Remarkably, nucleosome occupancy measured as histone H3 abundance relative to input DNA was comparable between C2S1 and *hog1-7* but almost totally lost in *ddm1-12*. This should be considered when interpreting the relative enrichment or depletion of histone marks in the mutants (Figure 3D, blue columns).

Mutations in *DDM1* or *HOG1* Affect Methylation of DNA and Histones Globally

Transcriptional silencing associated with DNA methylation and heterochromatic marks can be released by different means, including specific inhibitors or loss of function of epigenetic regulators. As shown above, the silent *HPT* transgene that was found in the polyploid lines did not respond to inhibitors. It also remained suppressed in the background of many mutations representing the known epigenetic regulatory pathways (Milos, 2006; Baubec et al., 2009; Foerster, 2009). This raised the question of why and how the new mutations in *DDM1* and *HOG1* proved to be exceptions and whether this could hint at an underlying mechanism. Both mutants have been reported to interfere with transcriptional gene silencing at many other targets in the *Arabidopsis* genome (Lippman et al., 2004; Jordan et al., 2007), but many of these were also expressed in those other mutants that did not reactivate the *HPT* gene. However, mutations in *DDM1* and *HOG1* have in common that they reduce DNA methylation and heterochromatic histone modifications at the *HPT* transgene. This effect of *DDM1* loss has also been described for other targets (Gendrel et al., 2002; Johnson et al., 2002; Soppe et al., 2002; Probst et al., 2003). Mutations in *HOG1* cause DNA hypomethylation at transgenic and endogenous repeats (Furner et al., 1998; Rocha et al., 2005; Mull et al., 2006), and the function of the *HOG1* gene regulating the level of the methyl group donor SAM suggested that its loss would also affect histone methylation (Rocha et al., 2005). To challenge the hypothesis that removal of both marks is a common feature of *ddm1* and *hog1*, we characterized DNA methylation and histone methylation in the novel mutant alleles in general and also at other sequences to allow for a direct comparison of the extent and specificity of the effects.

In agreement with results published for other alleles (Vongs et al., 1993; Furner et al., 1998; Jeddeloh et al., 1999; Rocha et al., 2005), global DNA methylation in *hog1-7* and *ddm1-12* was reduced to 2.7% (±0.47) and 1.7% (±0.13), respectively, in comparison to 5-methyldeoxycytosine (5-mdC) levels of 5.9% (±0.5) in the parental line C2S1, which is similar to wild-type levels (Rozhon et al., 2008) (Figure 4A). A significant proportion of the DNA methylation in wild-type *Arabidopsis* is found at repetitive sequences (Martinez-Zapater et al., 1986) and disappears in *ddm1* or *hog1* mutants (Vongs et al., 1993; Furner et al., 1998). This is also true for the new alleles: DNA gel blot analysis of DNA methylation at centromeric 180-bp repeats (Figure 4B) showed drastic hypomethylation in both mutants. However, the demethylation was more pronounced in the *ddm1-12* mutant, especially for the CG sites (Figure 4B). A certain difference was also evident after cytological analysis of the usually compact heterochromatic chromocentres by immunofluorescence, revealing dispersed 5-mdC localization in *ddm1-12*, where just 14% ($n = 104$) of nuclei retained chromocentric 5-mdC signals (Figure 4C). This is in agreement with other reports (Soppe et al., 2002). Nuclei of *hog1-7*, however, maintained most 5-mdC (89%, $n = 80$) at the chromocenters (CCs), close to wild-type nuclei (91%, $n = 109$), in accordance with the DNA gel blot methylation analysis of the centromeric repeats. This suggests that loss of DNA methylation in the *hog1-7* mutant occurs primarily at other parts of the genome. H3K9me2, as revealed by immunostaining, also colocalizes with CCs in wild-type nuclei (71%, $n = 129$) but is reduced in both mutants to 8 and 10% of nuclei having wild-type morphology ($n = 114$ and 107, respectively; Figure 4D), as also previously reported for *ddm1* (Probst et al., 2003).

The loss of chromocentric H3K9me2 signals in *hog1-7* nuclei, independent of the remaining DNA methylation, suggests a direct effect of SAM depletion on histone methylation. The cytological evidence was further substantiated by loss of silencing accompanied by reduced DNA and histone methylation at the retrotransposon without long terminal repeats *LINE1-4* (At2g01840) (Lippman et al., 2003) in the *ddm1-12* and *hog1-7* mutations (see Supplemental Figures 3A to 3C online), as well as by decreased levels of H3K9me2 and H3K4me3 in *hog1-7* analyzed by immunoblot (see Supplemental Figure 3D online). This provides further evidence of globally reduced histone methylation in *hog1* mutants, independent of the Lys residue analyzed.

Inhibition of SAHH Interferes with Maintenance of paTGS

The similar but not identical consequences of mutations in *DDM1* and *HOG1* on general DNA and histone methylation let us postulate that their comparable and exclusive role among TGS mutants in the maintenance of paTGS would occur through directly and simultaneously affecting DNA and histone methylation at the HPT promoter. A genetic approach to simultaneously reduce histone methylation and DNA methylation in all sequence contexts would require combination of at least six mutations and renders plants with severe developmental aberrations (Chan et al., 2006; Johnson et al., 2008). Therefore, we tried to mimic the *hog1* mutation by applying the specific SAHH inhibitor dihydroxypropyladenine (DHPA). The adenosine homolog DHPA was shown to induce hypomethylation and release of posttranscriptionally silenced transgenes in tobacco (*Nicotiana*

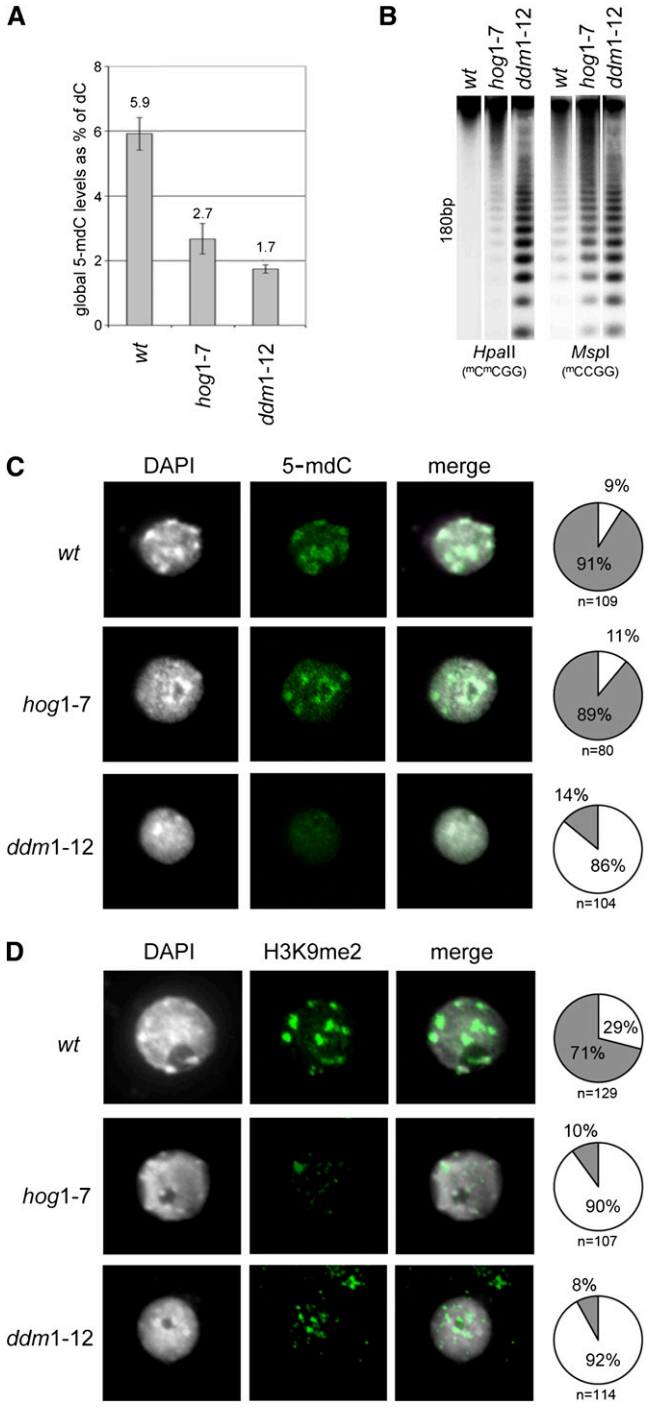

Figure 4. Mutations in *HOG1* and *DDM1* Lead to a Global Decrease of DNA and Histone Methylation.

(A) Global 5-mdC levels measured by HPLC are reduced in *hog1-7* and *ddm1-12* seedlings.

(B) DNA gel blot analysis showing decreased DNA methylation at centromeric 180-bp repeats in *hog1-7* and *ddm1-12* mutant plants.

(C) Chromocentric 5-mdC localization measured by immunofluorescence is lost only in *ddm1-12* but not in *hog1-7*. DAPI, 4',6-diamidino-2-phenylindole.

tabacum; Kovarik et al., 1994, 2000a). We first established the applicable dose range in *Arabidopsis* and analyzed the effectiveness of DHPA by germinating and growing seeds of a line with a transcriptionally silent, highly repetitive β-glucuronidase (GUS) transgene insertion on chromosome III (L5) (Morel et al., 2000) that is reactivated in the background of numerous epigenetic mutations (Elmayan et al., 2005), including *hog1-7* and *ddm1-12*, or by treatment with DNA methylation inhibitors (Baubec et al., 2009). DHPA treatments had only mild growth effects at the applied concentrations of 50 to 200 μM but successfully induced transcriptional reactivation of the GUS transgene (see Supplemental Figures 4A and 4B online). We subsequently compared DHPA inhibitors with drugs that change either DNA or histone modification. There is no inhibitor that specifically reduces histone methylation while leaving DNA methylation undisturbed. Thus, we applied the histone deacetylation inhibitor TSA, which has repeatedly been shown to convert silent into transcriptionally active genes (Chen and Pikaard, 1997; Xu et al., 2005). ZEB interferes specifically with DNA methylation (Zhou et al., 2002). We performed a side-by-side comparison of wild-type seedlings grown for 3 weeks on media containing either TSA, ZEB, or DHPA in the previously established dose ranges (Chang and Pikaard, 2005; Baubec et al., 2009; this article). We first analyzed transcriptional activation of endogenous repeats by quantitative real-time PCR. As observed in the mutant background (see Supplemental Figures 3A and 3B online), the retrotransposon without long terminal repeats *LINE1-4* (At2g01840) showed significant and dose-dependent transcript abundance (Figure 5A) and DNA hypomethylation (Figure 5B) after ZEB or DHPA, but not TSA treatments. Corresponding to the degree of transcriptional activation, we observed a significant, though not complete, reduction of H3K9me2 (Figure 5C). The active mark H3K4me3 increased but did not reach the levels seen in *ddm1* mutants (see Supplemental Figure 3C online). This is plausible since both histone modifications are likely to require SAM, which is a limiting factor in *hog1* and upon DHPA but not in *ddm1*. Data describing expression, DNA methylation, and histone modification for two other genomic sequences and cytological analysis of treated nuclei support the findings (see Supplemental Figures 5 and 6 online).

Although the retroelement *LINE1-4*, other repetitive sequences, and the second promoter of the transgene were transcriptionally activated by ZEB alone, silencing at the *HPT* promoter itself was not released by this drug (Figure 1B). Therefore, we evaluated the effects of DHPA treatments on expression, DNA methylation, and histone modification of the silenced *HPT* gene, asking whether the drugs would mimic the effects of the *hog1* mutation and release paTGS. The answer was affirmative, and high concentrations (200 μM) of SAHH inhibitor resulted in *HPT* expression up to 60% of the level in the hygromycin-resistant line C2R (Figure 6A). RNA gel blots with specific probes

(D) H3K9me2 compaction measured by immunofluorescence is disrupted in both mutants. The pie charts represent the percentage of nuclei with corresponding morphology. Gray, compact signals; white, dispersed signals.

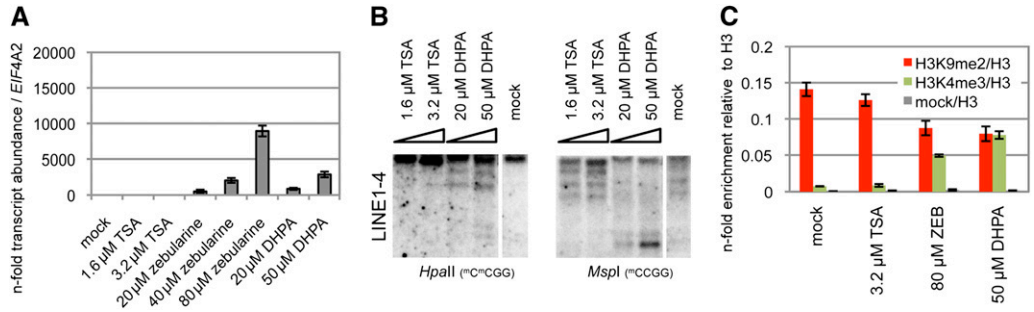

Figure 5. The SAHH Inhibitor DHPA Interferes with Transcriptional Gene Silencing at *LINE1-4.*

(A) Quantitative RT-PCR measuring the abundance of *LINE1-4* mRNA after chromatin drug and SAHH inhibitor treatments. Error bars denote SD from triplicate analyses.

(B) DNA gel blot analysis of DNA methylation with *LINE1-4*–specific probes after chromatin drug and SAHH inhibitor treatments.

(C) ChIP analysis of H3K9me2 (red) and H3K4me3 (green) histone modifications after chromatin drug and SAHH inhibitor treatments. Gray columns denote samples precipitated without antibodies.

[See online article for color version of this figure.]

revealed that both promoters were activated concordantly, with the primary promoter producing nearly as much *HPT* transcript as in the active state of the control line C2R (Figure 6B). DNA gel blot analysis of DNA methylation indicated dose-dependent hypomethylation at both promoters upon DHPA treatment, with CHG methylation more affected than CG (Figure 6C). This is in accordance with gradual demethylation at the *Hpa*II/*Msp*I recognition sequence $^{m}C^{m}CGG$ sites after DHPA treatments (Kovarik et al., 2000b). Quantification of histone modifications at the *HPT* promoter after DHPA treatments revealed loss of H3K9me2 and a slight gain of H3K4me3 already after 50 μM DHPA treatments (Figure 6D), as in *hog1-7*. In summary, the chemical interference produced by DHPA application has a similar effect as the genetically determined decrease of functional SAHH by the *hog1-7* mutation. Both cause a reduction of methylation of DNA and the associated histones of several genomic sequences, including the *HPT* transgene that underwent polyploidy-associated gene silencing. The lack of *HPT* reactivation upon depletion of only one type of methylation, in contrast with its restored transcription upon interference with both modifications simultaneously, suggests that this epiallele, and probably similar ones, are under a double-safeguard control that renders gene suppression extremely stable against epigenetic perturbation (Figure 7).

DISCUSSION

An undisputed definition of epigenetic inheritance is still lacking, but most descriptions refer to its reversible nature to distinguish it from genetic alterations inscribed in the DNA sequence. As is often the case in biology, this sharp distinction does not hold upon closer inspection. While many epigenetically regulated genes undergo programmed, regular, or random cycles of activation and suppression in the course of development, others have proven to be extremely stably silenced. Among them are many transposable elements, for which redundant control by different DNA methyltransferases (Kato et al., 2003) or a special reinforcement by small RNA silencing in the germ line (Brennecke et al., 2008; Slotkin et al., 2009) have been described. However, even transposons exhibit a surprising diversity in response to epigenetic interference in *Arabidopsis* where the role of well-defined epigenetic pathways can be studied in numerous mutants. Loss-of-function of DNA methyltransferases, argonaute proteins, histone methyltransferases, or histone deacetylases causes transcriptional activation of overlapping but not identical subsets of elements (Lippman et al., 2003). Most of these elements can also be activated by drugs that reduce either DNA methylation or histone modifications (Chang and Pikaard, 2005). Here, we have described a case of epigenetic transcriptional silencing that is surprisingly resistant to genetic and chemical interference, since removing one chromatin modification alone does not restore transcriptional activity from the potentially strong viral P35S promoter. Based on results from forward and reverse mutational screens (Milos, 2006; Baubec, 2008; Foerster, 2009), complemented by inhibitor experiments, we have provided evidence that two epigenetic features, namely, symmetric DNA methylation and histone methylation, cooperate to generate a double safeguard system that controls transcriptional suppression. Hence, both modifications have to be unlocked to convert the silent epiallele into an active one.

This could be achieved by a loss of functional DDM1, a member of the SWI2/SNF2 chromatin remodeling ATP-dependent helicase family. Mutations in *DDM1* known to decrease DNA methylation (Vongs et al., 1993; Kakutani et al., 1996, 1999) also reduce the levels of histone H3 dimethylation at Lys-9 (Gendrel et al., 2002; Habu et al., 2006). A partial interdependence of DNA methylation and H3K9me2 in *Arabidopsis* was further described in mutants of other genes whose products were supposed to act primarily on either DNA or H3K9 methylation (Johnson et al., 2002; Soppe et al., 2002; Tariq et al., 2003). These studies reveal a complex and possibly mutual interplay of DNA and histone methylation at different targets that can also depend on transcriptional activity. However, this interdependence does not apply to the silencing described in this study, since DNA or histone methyltransferase mutations alone did not reactivate the silent epiallele in our study. Even the concomitant reduction of

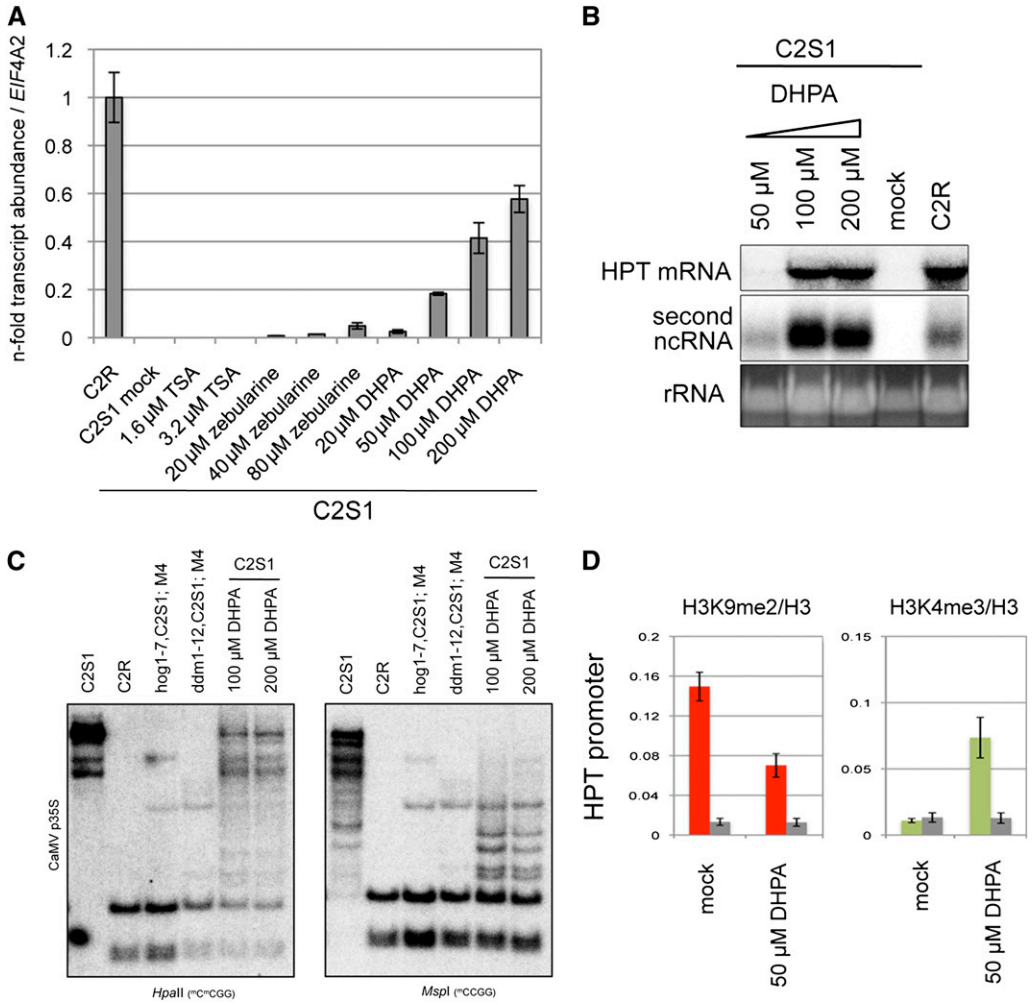

Figure 6. The SAHH Inhibitor DHPA Interferes with Maintenance of paTGS at the HPT Transgene.

(A) and **(B)** *HPT* transcript abundance in the inactive line C2S1 is significantly increased after treatments with DHPA.
(C) Increasing levels of DHPA lead to hypomethylation of the P35S promoters at the silent *HPT* transgene.
(D) The levels of H3K9 dimethylation (red) and H3K4 trimethlyation (green) at the P35S promoter changed after SAHH inhibitor treatments. Error bars in **(A)** and **(D)** denote SD from triplicate analyses.
[See online article for color version of this figure.]

both modifications was effective only above a certain threshold: mutant allele *ddm1-5*, isolated based on its strong reactivation of a transcriptionally silent HPT repeat (Mittelsten Scheid et al., 1998; Jeddeloh et al., 1999) but probably not a complete loss-of-function mutation (this study), did not evoke significant hygromycin resistance before the third inbred homozygous generation. Significant activity of the primary P35S promoter in the first homozygous mutant generation was only obtained with the three new *DDM1* mutations that disrupt the conserved regions of the protein and are likely more deleterious. While numerous previously mentioned studies describe the large-scale consequences of *ddm1* mutations for gene expression, transposon activation, and diverse chromatin modifications, the mechanistic connection between these effects and the remodeling activity of the protein extrapolated from in vitro experiments (Brzeski and Jerzmanowski, 2003) still remains to be uncovered. In this context, it is interesting that we observed decreased nucleosome abundance in DDM1-deficient plants. This could link the nucleosome remodeling function of DDM1 to the maintenance of DNA and histone methylation by facilitating a permissive environment for DNA and histone methyltransferases. Since *ddm1* is frequently investigated in the context of histone modifications (Gendrel et al., 2002; Lippman et al., 2004; Habu et al., 2006), lower nucleosome occupancy should be considered in quantitative comparisons.

By contrast, *hog1* mutations have so far only been analyzed for their effects on specific targets (Rocha et al., 2005; Mull et al., 2006) and general gene expression (Jordan et al., 2007). Nevertheless, the precise functional annotation of the gene product and the biochemical evidence for its role in regulating SAH levels

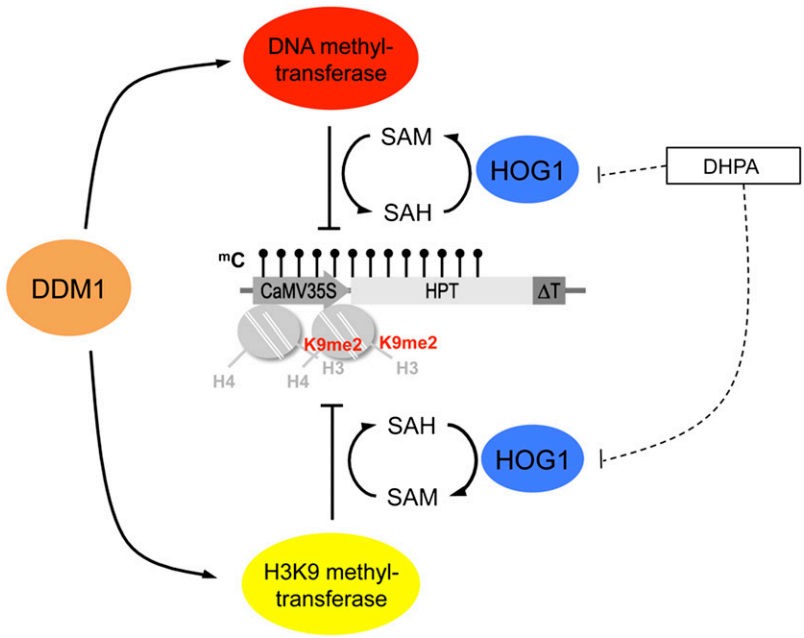

Figure 7. Cooperation of Multiple Chromatin Modifications to Generate Exceptional Stability of Silencing That Can Only Be Overcome by Simultaneous Removal of DNA Methylation (Black Lollipops) and Repressive Histone Modifications (Dimethylation at Lys-9 of histone H3).

The chromatin remodeling enzyme DDM1 and the *S*-adenosyl homocysteine hydrolase HOG1/SAHH are required to maintain both modifications, and only their lack in *ddm1* or *hog1* mutant or reduction of the methyl group donor SAM upon inhibitor application (DHPA) can release the tight double lock. [See online article for color version of this figure.]

(Rocha et al., 2005) make it easier to speculate about its mode of action. The methyl group donor SAM is a central hub for numerous methylation reactions modifying DNA, proteins, and metabolites (Roberts and Selker, 1995; Loenen, 2006; Roje, 2006). Therefore, substrate competition by even slightly increased SAH levels is expected to change many reactions simultaneously. The focus of HOG1 analysis has so far been on DNA as a methylation acceptor (Furner et al., 1998; Rocha et al., 2005), especially since changes in histone methylation levels were not detected in a weak *hog1* allele termed *sah*1L459F (Mull et al., 2006). Nevertheless, the new *hog1* allele brings about a substantial loss of H3K9me2 from CCs despite only slight decrease in DNA methylation, as well as a globally reduced methylation at several histones (though to different degrees). Furthermore, the mutant effects of transcriptional activation of the *HPT* transgene and endogenous transposable elements can be mimicked with a specific SAHH inhibitor. Together, these findings indicate that HOG1 is indeed a central factor in chromatin modification. This is further emphasized by the relatively small overlap of gene expression changes between *hog1-1* and treatment with the inhibitor 5-azacytidine (Jordan et al., 2007) that reduces DNA methylation and probably also 5-mdC–dependent histone methylation. Changing expression of many more genes indicates that *hog1* acts through interference with additional components. A central role of HOG1 for the plant as a whole is also evident from the severe phenotypic consequences of even subtle mutations and the embryonic lethality observed in loss-of-function mutants (Rocha et al., 2005). Due to the central role of SAM, there are probably many more, non-chromatin-related factors involved. It should be emphasized that the SAM:SAH ratio may also be modified by metabolic regulation or by sulfur availability (Nikiforova et al., 2006). Thus, the dependence of several chromatin components on the levels of SAM and SAH offers a path by which environmental or nutritional cues can inscribe a signature in the epigenetic outfit of the genome.

The forward genetic screen for reactivation of the *HPT* allele resulted in only 21 primary mutant candidates, surprisingly few for a mutant population derived from 20,000 independent T-DNA transformation events compared with other screens following insertional mutagenesis (Budziszewski et al., 2001). In addition, several candidates turned out to carry mutations within the marker gene itself (A. Foerster, unpublished data). This, together with finding three alleles of the *DDM1* gene, indicates saturation of the screen for *trans*-acting mutations. The mechanism of epigenetic control depicted in the double lock model makes these results nevertheless plausible: the need to eliminate two different chromatin modifications simultaneously requires either rare double mutations in two independent pathways or single mutations affecting the two modifications equally, making the screen a very stringent quest for strong modifications. Although very different in their assumed mode of action, DDM1 and HOG1 fulfill the latter conditions. Therefore, the double lock model is not only supported by the molecular data, but also by the general outcome of the forward screen.

It could be asked whether the data presented here, based mainly but not exclusively on the *HPT* transgene, have relevance

beyond this particular situation. The advantage of this experimental system is that it represents a gene whose activity is absolutely nonessential for the plants unless under selection and thereby does not bias the propagation or segregation of either the active or inactive states. It is inserted in an intergenic region (Mittelsten Scheid et al., 2003) and is therefore unlikely to cause an insertional mutation. The random rearrangement producing a duplication of the P35S promoter during the initial transformation event even allowed these two regulatory elements to be compared, with the surprising result that the identical sequences, in the same genomic location and with a distance of only 2 kb between them, respond quite differently to mutations and inhibitor effects. As pointed out before (Rocha et al., 2005), the silencing system in plants was not invented to inactivate man-made transgenes. Along this line, we demonstrated a clear epigenetic effect of the SAHH inhibitors and the *hog1* and *ddm1* mutant alleles on individual endogenous targets. A significant overlap of genes differentially regulated in both mutants, mainly but not exclusively transposons (T. Baubec and O. Mittelsten Scheid, unpublished data) further indicates more sequences under double control and a significant relevance of tight silencing beyond the *HPT* transgene.

More important is thinking about the role of polyploidy in generating a stable epiallele. While a diploid progenitor line containing the very same transgene always maintained high expression, partial or complete silencing was found in several independent autotetraploid derivatives (Mittelsten Scheid et al., 2003). However, these were generated by protoplast culture and regeneration, leaving other parameters, such as hormone effects, tissue culture conditions, or even propagation of preexisting epigenetic states in individual cells, as possible sources of silencing, rather than polyploidization. Nevertheless, an association with polyploidy is very likely based on the *trans*-acting silencing between inactive and active epialleles, which is limited to tetraploid hybrids (Mittelsten Scheid et al., 2003), and with a specific set of genes that are differentially expressed in the tetraploid lines. Although gene expression changes in autotetraploids are less frequent compared with freshly formed allopolyploids (Wang et al., 2004), polyploidization is recognized as being a significant source of genetic as well as epigenetic changes in many different plant species (for review, see Osborn et al., 2003; Adams and Wendel, 2005). paTGS can apparently generate very tightly controlled epialleles with an extremely low frequency of reversion and with the potential to be propagated and even spread among plant populations. It should be considered to be an important source of epigenetic diversity with an evolutionary impact.

METHODS

Plant Growth and Chemical Treatments

Stratified seeds were surface-sterilized with 5% sodium hypochlorite and 0.05% Tween 80 for 6 min and washed and air-dried overnight. Sterilized seeds were germinated and grown in Petri dishes containing agar-solidified germination medium in growth chambers under 16-h-light/8-h-dark cycles at 21°C. For treatments with hygromycin (Calbiochem), TSA (Sigma-Aldrich), ZEB (Sigma-Aldrich), and DHPA (donated by Ales Kovarik), seeds were sown and grown directly on drug-containing plates under the conditions described above. Hygromycin (10 μg/mL), zebularine (20, 40, and 80 μM), and DHPA (50, 100, and 200 μM) in aqueous solution or TSA (1.6 and 3.2 μM) dissolved in DMSO were added to the germination medium before solidifying.

Mutant Screen and Mapping

Diploid C2S1 plants (in the background of accession Zürich) were mutagenized by random T-DNA insertion after *Agrobacterium tumefaciens* transformation with p1'barbi (Mengiste et al., 1997). M2 seeds from 20,000 mutant M1 plants were harvested in pools of 15 M1 plants and selected on hygromycin-containing medium. *HPT*-expressing and non-expressing lines, C2R and C2S1, were used as positive and negative controls, respectively. Hygromycin-resistant plants were further propagated, and hygromycin resistance was followed in subsequent generations after selfing and outcrossing to the wild type. Sequences flanking the T-DNA insertion that were genetically linked with the mutations (*ddm1-13* and *hog1-7*) were identified by thermal asymmetric interlaced PCR as described (Liu et al., 1995). Other mutations were identified by sequencing of candidate genes (as in the case of *ddm1-11* and *ddm1-12*).

Nucleic Acid Isolation and Gel Blot Analysis

Pools of 50 to 100 seedlings (age as indicated for the individual experiments) were shock-frozen in liquid nitrogen, homogenized, and subsequently used for DNA or RNA extraction using Phytopure (Amersham) or RNAeasy (Qiagen) kits, respectively.

For DNA methylation analysis by DNA gel blot, 10 μg of genomic DNA were digested overnight with 1 to 2 units of *Hpa*II (sensitive to ^{m}C^{m}CGG) or *Msp*I (sensitive to ^{m}CCGG) restriction enzymes. Subsequently, samples were electrophoretically separated on TAE agarose gels, depurinated for 10 min in 250 mM HCl, denatured for 30 min in 0.5 M NaOH and 1.5 M NaCl, and neutralized twice in 0.5 M Tris, 1.5 M NaCl, and 1 mM EDTA at pH 7.2 for 15 min. For RNA gel blot analysis, 10 μg of total RNA were denatured with 15% glyoxal and DMSO for 1 h at 50°C and separated on 1.4% agarose gels in 10 mM sodium phosphate buffer, pH 7.0, in a Sea2000 circular flow electrophoresis chamber (Elchrom Scientific). DNA and RNA gels were blotted onto Hybond N^{+} membranes (GE Healthcare) overnight with 20× SSC and washed, and the samples were UV cross-linked using a Stratalinker (Stratagene). Hybridization was performed as described (Church and Gilbert, 1984). Radioactively labeled sequence-specific probes were synthesized from 25 ng of template DNA in the presence of 50 μCi of [α-^{32}P]dCT- (Hartmann Analytic) using the Rediprime labeling kit (Amersham). Signals of exposures in the linear range were detected with phosphor imager screens (Bio-Rad) and scanned with a Molecular Imager FX (Bio-Rad).

Quantification of Global DNA Methylation

Total cytosine methylation was determined by cation exchange HPLC as described by Rozhon et al. (2008). All samples were analyzed in triplicate, and 5-mdC values were expressed as a percentage of total cytosine.

Reverse Transcription and Quantitative Real-Time PCR

RNA samples were treated with 5 units of DNase I (MBI Fermentas), 0.4 units of RNasin, and 4 μL of 10× DNase I buffer for 40 min at 37°C to remove residual DNA contamination, extracted with phenol:chloroform (24:1), and subsequently ethanol-precipitated. Reverse transcription was performed on 1 μg of RNA with 0.2 μg of random hexamer primers (MBI Fermentas) using 1 unit of RevertAid H Minus M-MuLV-RTase (MBI Fermentas) at 42°C for 11/2 h. Real-time PCR analysis was performed with the 2× SensiMix Plus SYBR and Fluorescein Kit (Quantace) protocol

using an iQ5 real-time PCR system (Bio-Rad Laboratories). Ct values were analyzed using Excel (Microsoft). The primer sequences are listed in Supplemental Table 1 online.

In Situ GUS Detection

GUS activity was detected by staining plant tissue in 0.1 M sodium phosphate buffe, pH 7.0, 10 mM EDTA, 0.1% Triton X-100, 100 μg/mL chloramphenicol, 2 mM potassium ferrocyanide, 2 mM potassium ferricyanide, and 0.5 mg/mL X-glucuronide after 30 min vacuum infiltration and overnight incubation at 37°C. Subsequent washes with 70% ethanol at 37°C were performed to remove chlorophyll and enhance contrast. All samples were analyzed using a Leica MZ16FA binocular microscope with a Leica DFC300FX CCD camera. Images were acquired with the Leica Application Suite and processed with Adobe Photoshop (Adobe).

Immunofluorescence

For the preparation of nuclei, 21-d-old plantlets were rinsed in 10 mM Tris buffer, pH 7.5, fixed by vacuum infiltration in 4% formaldehyde/Tris buffer, rinsed in Tris buffer, chopped in 500 μL chromosome isolation buffer (15 mM Tris, 2 mM Na_2EDTA, 0.5 mM spermin, 80 mM KCl, 20 mM NaCl, 15 mM β-mercaptoethanol, and 0.1% Triton X-100, pH 7.5), and filtered through a 50-μm nylon mesh. Fifty microliters of suspension was transferred onto microscope slides, and nuclei were attached to the slide using a cytospin centrifuge (MPW) at 2500 rpm for 10 min.

Immunolocalization of methylated cytosine was performed as described (Jasencakova et al., 2000), with minor modifications. In brief, slides were treated with pepsin (50 μg/mL in 0.01 M HCl; Roche) at 38°C (1 to 2 min), postfixed in 4% formaldehyde/2× SSC, denatured in 70% formamide/2× SSC at 80°C (2 min), and cooled in ice-cold 1× PBS. After blocking (5% BSA, 0.2% Tween 20, and 4× SSC) at 37°C (30 min), the slides were incubated with primary monoclonal mouse-anti-5-methylcytosine (Eurogentec) and secondary goat-anti-mouse-Alexa488 (Molecular Probes) antibodies. Immunolocalization of histone H3 modifications was performed as previously described (Jasencakova et al., 2000). Slides were fixed in 4% paraformaldehyde/PBS for 20 min and blocked (5% BSA, 0.2% Tween 20, and 4× SSC) at 37°C (30 min). The slides were incubated overnight at 4°C with primary antibodies specific to H3K9me2 (T. Jenuwein; 4677) and secondary goat-anti-rabbit-AF488 (Molecular Probes). The slides were counterstained with 4',6-diamidino-2-phenylindole (Vector Laboratories) and analyzed using a Zeiss Axioplan 2 epifluorescence microscope. Monochromatic images were acquired with MetaVue (Universal Imaging) and processed with Adobe Photoshop (Adobe).

Bisulfite Conversion, Sequencing, and Evaluation

After treatment with RNase A and proteinase K, 1 to 2 μg of genomic DNA were digested overnight with *Bam*HI (MBI Fermentas). Subsequent bisulfite conversion was performed using the Epitect conversion kit (Qiagen) and controlled for completion as described (Hetzl et al., 2007). Converted DNA was used for PCR amplification (see Supplemental Table 1 online). PCR-amplified DNA was cloned using CloneJet (MBI Fermentas) and ligation mixes transformed into DH5α cells (Invitrogen), sequenced by terminal labeling using BigDye Terminator v3.1 (Applied Biosystems), and read at vbcgenomics.com. The sequence information obtained was analyzed with CyMATE (www.gmi.oeaw.ac.at/cymate; Hetzl et al., 2007) and Excel (Microsoft).

ChIP

ChIP was performed as described (www.epigenome-noe.net/researchtools/protocol.php) using 3-week-old seedlings. The chromatin was immunoprecipitated with antibodies to histone H3 (Abcam; ab1791), H3K4me3 (Upstate; 07-473), H4pentaAc (Millipore; P62805), H3K9me2 (T. Jenuwein, 4677; Abcam, ab1220). Immunoprecipitated DNA was purified using a Qiagen PCR purification kit and eluted in 50 μL of EB buffer. Quantitative real-time PCR was performed in a total reaction volume of 25 μL, and quantitative PCR conditions were according to the 2× SensiMix Plus SYBR and Fluorescein kit (Quantace) protocol using an iQ5 real-time-PCR system (Bio-Rad Laboratories). Quantitative PCR data were evaluated as a ratio either to input DNA or to H3 abundance (Haring et al., 2007), as indicated.

Immunoblot Analysis

Immunoblot analysis was performed as described (Yan et al., 2007). Approximately 20 μg per sample were loaded on 15% SDS-PAGE gels and subsequently blotted onto polyvinylidene fluoride membranes (Amersham). The primary antibodies were H3 (Abcam; ab1791), H3K9me2 (T. Jenuwein; 4677), and H3K4me3 (Upstate; 07-473); the secondary antibody was peroxidase-conjugated goat-anti-rabbit (Jackson Immuno Research). Detection was performed using Lumi-Light protein gel blotting substrate (Roche).

Accession Numbers

Sequence data from this article can be found in the Arabidopsis Genome Initiative or GenBank/EMBL databases under the following accession numbers: *DDM1*, At5g66750; *SAHH1*, At4g13940; *SAHH2*, At3g23810; *LINE1-4*, At2g01840; *EIF4A2*, At1g54270; and *TUBULIN8*, At5g23860.

Author Contributions

The experiments were designed by T.B. and O.M.S. and performed by T.B. (main), A.P. (cytology), B.R. (protein gel blot), W.R. (global cytosine methylation), and B.W. (mutant screen). The data were analyzed by T.B., H.Q.D., A.v.H., and O.M.S. The article was written by T.B. and O.M.S.

Supplemental Data

The following materials are available in the online version of this article.

Supplemental Figure 1. *HPT* Transcript Abundance in Zebularine- and Mock-Treated Wild-Type and Mutant Plants.

Supplemental Figure 2. Location and Organization of the *HPT* Transgenic Insert in the Short Arm of Chromosome III.

Supplemental Figure 3. Effects of *ddm1-12* and *hog1-7* on *LINE1-4* Silencing and Global Histone Modifications.

Supplemental Figure 4. Treatments with the SAHH Inhibitor DHPA Releases Silencing of Repetitive Transgenes.

Supplemental Figure 5. Treatment with the SAHH Inhibitor DHPA Reduces Levels of DNA and Histone Methylation at Endogenous Repeats.

Supplemental Figure 6. DHPA Treatment Reduces H3K9me2 but Not DNA Methylation at Chromocenters.

Supplemental Table 1. DNA Sequence of Primers Used throughout This Study.

ACKNOWLEDGMENTS

We thank Victor Marquez and Ales Kovarik for generous gifts of the SAHH inhibitors and Herve Vaucheret for line L5. The mutagenesis of C2S1 was performed in the lab and with support of Jerzy Paszkowski at the Friedrich Miescher Institute for Biomedical Research in Basel. We are grateful for the assistance of Markus Briker and Karin Afsar in

generating the mutant collection. We thank Barbara Hohn, Aline Probst, Andrea Förster-Sümecz, and three anonymous reviewers for helpful comments on the manuscript and Maria Siomos for valuable editorial input. The work was financially supported by the Austrian Academy of Sciences, Austrian Science Fund Grant P18986-B17, EU NoE "Epigenome" and GEN-AU GZ 200.140-VI/1/2006 to O.M.S., and the Vienna Science and Technology Fund to A.v.H.

Received November 15, 2009; revised December 15, 2009; accepted December 29, 2009; published January 22, 2010.

REFERENCES

Adams, K.L., and Wendel, J.F. (2005). Polyploidy and genome evolution in plants. Curr. Opin. Plant Biol. **8:** 135–141.

Baubec, T. (2008). Maintenance of polyploidy-associated transcriptional gene silencing in *Arabidopsis thaliana*, dissertation (Austria: University of Vienna). http://othes.univie.ac.at/3756/.

Baubec, T., Pecinka, A., Rozhon, W., and Mittelsten Scheid, O. (2009). Effective, homogeneous and transient interference with cytosine methylation in plant genomic DNA by zebularine. Plant J. **57:** 542–554.

Bork, P., and Koonin, E.V. (1993). An expanding family of helicases within the 'DEAD/H' superfamily. Nucleic Acids Res. **21:** 751–752.

Brennecke, J., Malone, C.D., Aravin, A.A., Sachidanandam, R., Stark, A., and Hannon, G.J. (2008). An epigenetic role for maternally inherited piRNAs in transposon silencing. Science **322:** 1387–1392.

Brzeski, J., and Jerzmanowski, A. (2003). Deficient in DNA methylation 1 (DDM1) defines a novel family of chromatin-remodeling factors. J. Biol. Chem. **278:** 823–828.

Budziszewski, G.J., et al. (2001). Arabidopsis genes essential for seedling viability: Isolation of Insertional mutants and molecular cloning. Genetics **159:** 1765–1778.

Chan, S.W.L., Henderson, I.R., Zhang, X.Y., Shah, G., Chien, J.S.C., and Jacobsen, S.E. (2006). RNAi, DRD1, and histone methylation actively target developmentally important non-CG DNA methylation in Arabidopsis. PLoS Genet. **2:** 791–797.

Chandler, V.L., Eggleston, W.B., and Dorweiler, J.E. (2000). Paramutation in maize. Plant Mol. Biol. **43:** 121–145.

Chang, S., and Pikaard, C. (2005). Transcript profiling in Arabidopsis reveals complex responses to global inhibition of DNA methylation and histone deacetylation. J. Biol. Chem. **280:** 796–804.

Chen, Z.J., and Pikaard, C.S. (1997). Epigenetic silencing of RNA polymerase I transcription: A role for DNA methylation and histone modification in nucleolar dominance. Genes Dev. **11:** 2124–2136.

Chen, Z.J., and Tian, L. (2007). Roles of dynamic and reversible histone acetylation in plant development and polyploidy. Biochim. Biophys. Acta **1769:** 295–307.

Chinnusamy, V., and Zhu, J.K. (2009). Epigenetic regulation of stress responses in plants. Curr. Opin. Plant Biol. **12:** 133–139.

Chong, S.Y., and Whitelaw, E. (2004). Epigenetic germline inheritance. Curr. Opin. Genet. Dev. **14:** 692–696.

Church, G.M., and Gilbert, W. (1984). Genomic sequencing. Proc. Natl. Acad. Sci. USA **81:** 1991–1995.

Cubas, P., Vincent, C., and Coen, E. (1999). An epigenetic mutation responsible for natural variation in floral symmetry. Nature **401:** 157–161.

Elmayan, T., Proux, F., and Vaucheret, H. (2005). Arabidopsis RPA2: A genetic link among transcriptional gene silencing, DNA repair, and DNA replication. Curr. Biol. **15:** 1919–1925.

Finnegan, E.J. (2002). Epialleles - A source of random variation in times of stress. Curr. Opin. Plant Biol. **5:** 101–106.

Foerster, A.M. (2009). Functional analysis of epialleles in diploid and tetraploid *Arabidopsis thaliana*, dissertation (Austria: University of Vienna). http://othes.univie.ac.at/7879/1/2009-10-27_0001330.pdf.

Fuchs, J., Demidov, D., Houben, A., and Schubert, I. (2006). Chromosomal histone modification patterns: From conservation to diversity. Trends Plant Sci. **11:** 199–208.

Furner, I.J., Sheikh, M.A., and Collett, C.E. (1998). Gene silencing and homology-dependent gene silencing in Arabidopsis: Genetic modifiers and DNA methylation. Genetics **149:** 651–662.

Gendrel, A.V., Lippman, Z., Yordan, C., Colot, V., and Martienssen, R.A. (2002). Dependence of heterochromatic histone H3 methylation patterns on the Arabidopsis gene DDM1. Science **297:** 1871–1873.

Habu, Y., Mathieu, O., Tariq, M., Probst, A.V., Smathajitt, C., Zhu, T., and Paszkowski, J. (2006). Epigenetic regulation of transcription in intermediate heterochromatin. EMBO Rep. **7:** 1279–1284.

Haring, M., Offermann, S., Danker, T., Horst, I., Peterhansel, C., and Stam, M. (2007). Chromatin immunoprecipitation: optimization, quantitative analysis and data normalization. Plant Methods **3:** 11.

Hetzl, J., Foerster, A.M., Raidl, G., and Mittelsten Scheid, O. (2007). CyMATE: A new tool for methylation analysis of plant genornic DNA after bisulphite sequencing. Plant J. **51:** 526–536.

Jasencakova, Z., Meister, A., Walter, J., Turner, B.M., and Schubert, I. (2000). Histone H4 acetylation of euchromatin and heterochromatin is cell cycle dependent and correlated with replication rather than with transcription. Plant Cell **12:** 2087–2100.

Jeddeloh, J.A., Stokes, T.L., and Richards, E.J. (1999). Maintenance of genomic methylation requires a SWI2/SNF2-like protein. Nat. Genet. **22:** 94–97.

Johnson, L.M., Cao, X.F., and Jacobsen, S.E. (2002). Interplay between two epigenetic marks: DNA methylation and histone H3 lysine 9 methylation. Curr. Biol. **12:** 1360–1367.

Johnson, L.M., Law, J.A., Khattar, A., Henderson, I.R., and Jacobsen, S.E. (2008). SRA-domain proteins required for DRM2-mediated de novo DNA methylation. PLoS Genet. **4:** e1000280.

Jordan, N.D., West, J.P., Bottley, A., Sheikh, M., and Furner, I. (2007). Transcript profiling of the hypomethylated hog1 mutant of Arabidopsis. Plant Mol. Biol. **65:** 571–586.

Kakutani, T., Jeddeloh, J.A., Flowers, S.K., Munakata, K., and Richards, E.J. (1996). Developmental abnormalities and epimutations associated with DNA hypomethylation mutations. Proc. Natl. Acad. Sci. USA **93:** 12406–12411.

Kakutani, T., Munakata, K., Richards, E.J., and Hirochika, H. (1999). Meiotically and mitotically stable inheritance of DNA hypomethylation induced by ddm1 mutation of *Arabidopsis thaliana*. Genetics **151:** 831–838.

Kalisz, S., and Purugganan, M.D. (2004). Epialleles via DNA methylation: Consequences for plant evolution. Trends Ecol. Evol. **19:** 309–314.

Kato, M., Miura, A., Bender, J., Jacobsen, S.E., and Kakutani, T. (2003). Role of CG and non-CG methylation in immobilization of transposons in Arabidopsis. Curr. Biol. **13:** 421–426.

Kovarik, A., Koukalova, B., Holy, A., and Bezdek, M. (1994). Sequence-specific hypomethylation of the tobacco genome induced with dihydroxypropyladenine, ethionine and 5-azacytidine. FEBS Lett. **353:** 309–311.

Kovarik, A., Koukalova, B., Lim, K.Y., Matyasek, R., Lichtenstein, C.P., Leitch, A.R., and Bezdek, M. (2000b). Comparative analysis of DNA methylation in tobacco heterochromatic sequences. Chromosome Res. **8:** 527–541.

Kovarik, A., Van Houdt, H., Holy, A., and Depicker, A. (2000a). Drug-induced hypomethylation of a posttranscriptionally silenced transgene locus of tobacco leads to partial release of silencing. FEBS Lett. **467:** 47–51.

Lippman, Z., et al. (2004). Role of transposable elements in heterochromatin and epigenetic control. Nature **430:** 471–476.

Lippman, Z., May, B., Yordan, C., Singer, T., and Martienssen, R. (2003). Distinct mechanisms determine transposon inheritance and methylation via small interfering RNA and histone modification. PLoS Biol. **1:** 420–428.

Liu, Y.G., Mitsukawa, N., Oosumi, T., and Whittier, R.F. (1995). Efficient isolation and mapping of *Arabidopsis thaliana* T-DNA insert junctions by thermal asymmetric interlaced PCR. Plant J. **8:** 457–463.

Loenen, W.A.M. (2006). S-adenosylmethionine: Jack of all trades and master of everything? Biochem. Soc. Trans. **34:** 330–333.

Madlung, A., and Comai, L. (2004). The effect of stress on genome regulation and structure. Ann. Bot. (Lond.) **94:** 481–495.

Martinez-Zapater, J.M., Estelle, M.A., and Somerville, C.R. (1986). A highly repeated DNA-sequence in *Arabidopsis thaliana*. Mol. Gen. Genet. **204:** 417–423.

Masterson, J. (1994). Stomatal size in fossil plants: Evidence for polyploidy in majority of angiosperms. Science **264:** 421–424.

Mathieu, O., Jasencakova, Z., Vaillant, I., Gendrel, A.V., Colot, V., Schubert, I., and Tourmente, S. (2003). Changes in 5S rDNA chromatin organization and transcription during heterochromatin establishment in Arabidopsis. Plant Cell **15:** 2929–2939.

Mengiste, T., Amedeo, P., and Paszkowski, J. (1997). High-efficiency transformation of Arabidopsis thaliana with a selectable marker gene regulated by the T-DNA 1' promoter. Plant J. **12:** 945–948.

Milos, M. (2006). A reverse genetic approach to analyse ploidy-associated gene silencing in *Arabidopsis thaliana*, dissertation (Austria: University of Vienna). http://othes.univie.ac.at/5529/.

Mittelsten Scheid, O., Afsar, K., and Paszkowski, J. (1998). Release of epigenetic gene silencing by trans-acting mutations in Arabidopsis. Proc. Natl. Acad. Sci. USA **95:** 632–637.

Mittelsten Scheid, O., Afsar, K., and Paszkowski, J. (2003). Formation of stable epialleles and their paramutation-like interaction in tetraploid *Arabidopsis thaliana*. Nat. Genet. **34:** 450–454.

Morel, J.B., Mourrain, P., Beclin, C., and Vaucheret, H. (2000). DNA methylation and chromatin structure affect transcriptional and post-transcriptional transgene silencing in Arabidopsis. Curr. Biol. **10:** 1591–1594.

Mull, L., Ebbs, M.L., and Bender, J. (2006). A histone methylation-dependent DNA methylation pathway is uniquely impaired by deficiency in Arabidopsis S-adenosylhomocysteine hydrolase. Genetics **174:** 1161–1171.

Nikiforova, V.J., Bielecka, M., Gakiere, B., Krueger, S., Rinder, J., Kempa, S., Morcuende, R., Scheible, W.R., Hesse, H., and Hoefgen, R. (2006). Effect of sulfur availability on the integrity of amino acid biosynthesis in plants. Amino Acids **30:** 173–183.

Ooi, S.K.T., and Bestor, T.H. (2008). The colorful history of active DNA demethylation. Cell **133:** 1145–1148.

Osborn, T.C., Pires, J.C., Birchler, J.A., Auger, D.L., Chen, Z.J., Lee, H.S., Comai, L., Madlung, A., Doerge, R.W., Colot, V., and Martienssen, R.A. (2003). Understanding mechanisms of novel gene expression in polyploids. Trends Genet. **19:** 141–147.

Pfluger, J., and Wagner, D. (2007). Histone modifications and dynamic regulation of genome accessibility in plants. Curr. Opin. Plant Biol. **10:** 645–652.

Probst, A.V., Fransz, P.F., Paszkowski, J., and Mittelsten Scheid, O. (2003). Two means of transcriptional reactivation within heterochromatin. Plant J. **33:** 743–749.

Rangan, L., Vogel, C., and Srivastava, A. (2008). Analysis of context sequence surrounding translation initiation site from complete genome of model plants. Mol. Biotechnol. **39:** 207–213.

Roberts, C.J., and Selker, E.U. (1995). Mutations affecting the biosynthesis of S-adenosylmethionine cause reduction of DNA methylation in *Neurospora crassa*. Nucleic Acids Res. **23:** 4818–4826.

Rocha, P., Sheikh, M., Melchiorre, R., Fagard, M., Boutet, S., Loach, R., Moffatt, B., Wagner, C., Vaucheret, H., and Furner, I. (2005). The Arabidopsis HOMOLOGY-DEPENDENT GENE SILENCING1 gene codes for an *S*-adenosyl-L-homocysteine hydrolase required for DNA methylation-dependent gene silencing. Plant Cell **17:** 404–417.

Roje, S. (2006). S-Adenosyl-L-methionine: Beyond the universal methyl group donor. Phytochemistry **67:** 1686–1698.

Rozhon, W., Baubec, T., Mayerhofer, J., Mittelsten Scheid, O., and Jonak, C. (2008). Rapid quantification of global DNA methylation by isocratic cation exchange high-performance liquid chromatography. Anal. Biochem. **375:** 354–360.

Slotkin, R.K., Vaughn, M., Borges, F., Tanurdzic, M., Becker, J.D., Feijo, J.A., and Martienssen, R.A. (2009). Epigenetic reprogramming and small RNA silencing of transposable elements in pollen. Cell **136:** 461–472.

Soppe, W.J.J., Jasencakova, Z., Houben, A., Kakutani, T., Meister, A., Huang, M.S., Jacobsen, S.E., Schubert, I., and Fransz, P.F. (2002). DNA methylation controls histone H3 lysine 9 methylation and heterochromatin assembly in Arabidopsis. EMBO J. **21:** 6549–6559.

Stebbins, G.L. (1966). Chromosomal variation and evolution. Science **152:** 1463–1469.

Tariq, M., Saze, H., Probst, A.V., Lichota, J., Habu, Y., and Paszkowski, J. (2003). Erasure of CpG methylation in Arabidopsis alters patterns of histone H3 methylation in heterochromatin. Proc. Natl. Acad. Sci. USA **100:** 8823–8827.

Vaillant, I., and Paszkowski, J. (2007). Role of histone and DNA methylation in gene regulation. Curr. Opin. Plant Biol. **10:** 528–533.

Vongs, A., Kakutani, T., Martienssen, R.A., and Richards, E.J. (1993). *Arabidopsis thaliana* DNA methylation mutants. Science **260:** 1926–1928.

Wang, J.L., Tian, L., Madlung, A., Lee, H.S., Chen, M., Lee, J.J., Watson, B., Kagochi, T., Comai, L., and Chen, Z.J. (2004). Stochastic and epigenetic changes of gene expression in Arabidopsis polyploids. Genetics **167:** 1961–1973.

Weretilnyk, E.A., Alexander, K.J., Drebenstedt, M., Snider, J.D., Summers, P.S., and Moffatt, B.A. (2001). Maintaining methylation activities during salt stress. The involvement of adenosine kinase. Plant Physiol. **125:** 856–865.

Xu, C.R., Liu, C., Wang, Y.L., Li, L.C., Chen, W.Q., Xu, Z.H., and Bai, S.N. (2005). Histone acetylation affects expression of cellular patterning genes in the Arabidopsis root epidermis. Proc. Natl. Acad. Sci. USA **102:** 14469–14474.

Yan, D., Zhang, Y., Niu, L., Yuan, Y., and Cao, X. (2007). Identification and characterization of two closely related histone H4 arginine 3 methyltransferases in *Arabidopsis thaliana*. Biochem. J. **408:** 113–121.

Yoshida, M., Horinouchi, S., and Beppu, T. (1995). Trichostatin A and trapoxin: Novel chemical probes for the role of histone acetylation in chromatin structure and function. Bioessays **17:** 423–430.

Zhou, L., Cheng, X., Connolly, B.A., Dickman, M.J., Hurd, P.J., and Hornby, D.P. (2002). Zebularine: A novel DNA methylation inhibitor that forms a covalent complex with DNA methyltransferases. J. Mol. Biol. **321:** 591–599.

Supplemental Figure 1

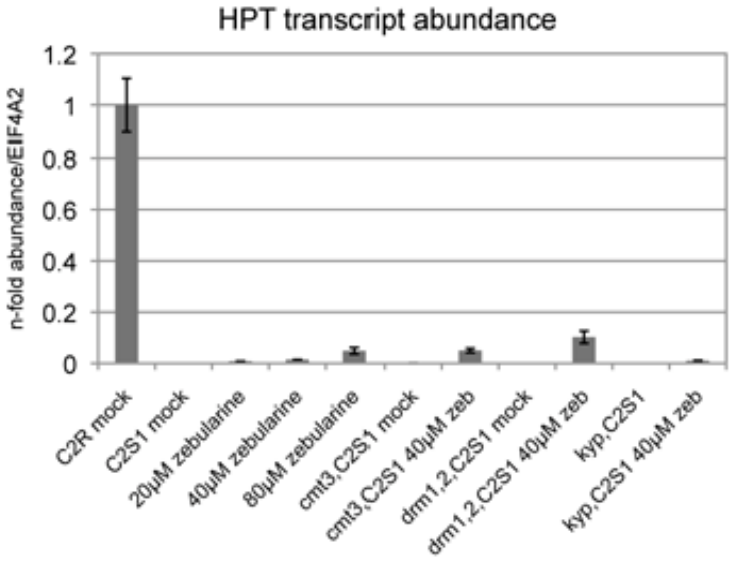

Supplemental Figure 1. HPT transcript abundance in zebularine- and mock-treated wild type and mutant plants.

Quantitative reverse-transcription PCR measuring abundance of *HPT* mRNA relative to *EIF4A2* after zebularine treatments and/or in *cmt3*, *drm1,2* or *kyp* mutant backgrounds. Error bars indicate standard deviation between triplicate analysis.

Supplemental Figure 2

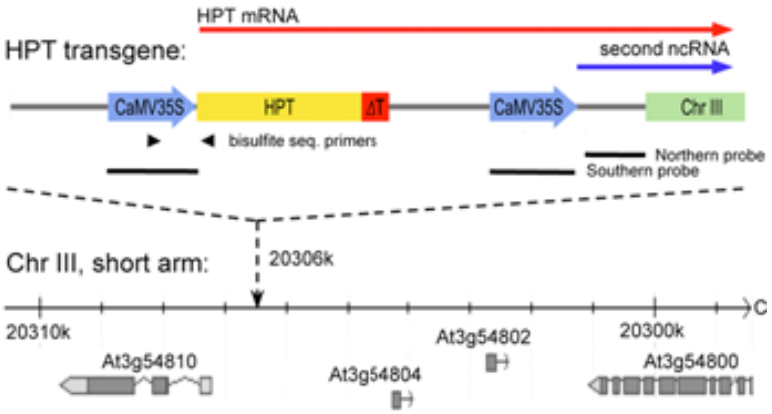

Supplemental Figure 2.

Location and organisation of the *HPT* transgenic insert in the short arm of chromosome III. *HPT* and nc-transcripts are indicated by red and blue arrows, respectively. Probes and primers used in subsequent experiments are indicated as black lines and arrowheads.

Supplemental Figure 3

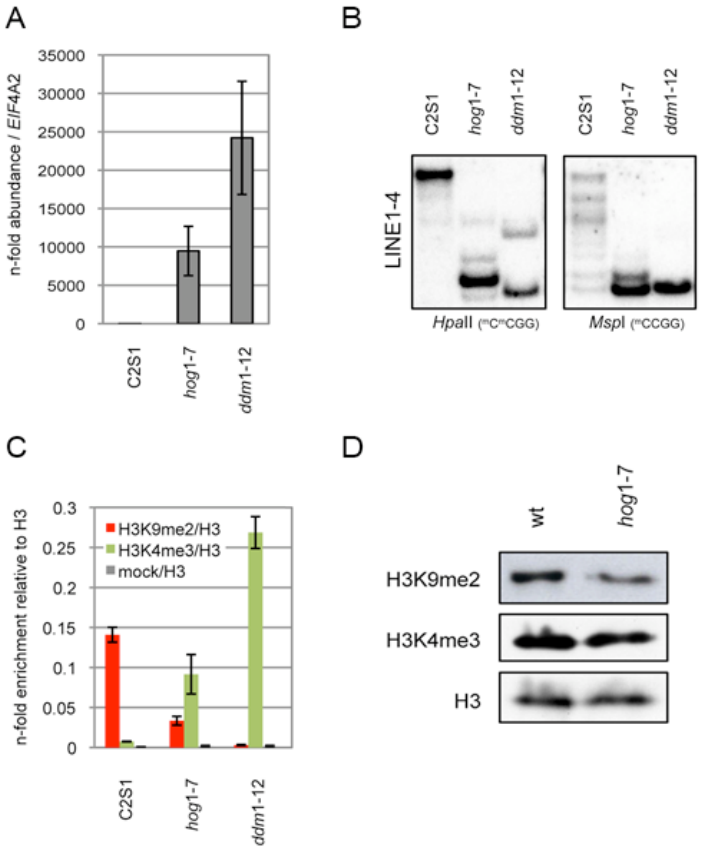

Supplemental Figure 3. Effects of *ddm1-12* and *hog1-7* on *LINE1-4* silencing and global histone modifications.

(A) Quantitative reverse-transcription PCR measuring abundance of *LINE1-4* mRNA in mutant background relative to *EIF4A2.*

(B) DNA methylation DNA blot analysis with *LINE1-4*-specific probes.

(C) Quantitative analysis of H3K9me2 (red) and H3K4me3 (green) enrichment normalised to histone H3 at *LINE1-4* by ChIP. Grey columns represent samples precipitated without antibodies.

(D) Immunoblot analysis of histone modifications at H3K9 and H3K4 in the *hog1-7* mutant compared to wild type. Error bars in (A) and (C) indicate standard deviation of triplicate analysis.

Supplemental Figure 4

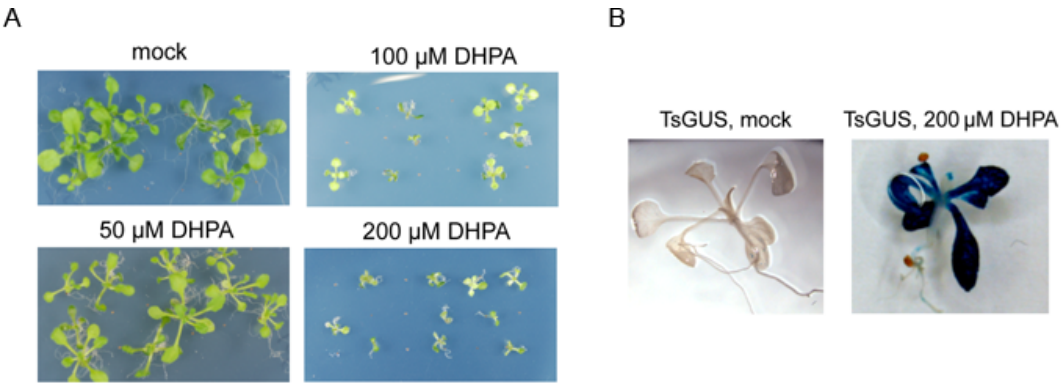

Supplemental Figure 4. Treatments with the SAHH inhibitor DHPA releases TS-GUS silencing.

(A) Growth analysis in the presence of the S-adenosyl-L-homocysteine hydrolase (SAHH) inhibitor DHPA at different concentrations using TS-GUS plants (L5, Morel., et al 2000).

(B) TS-GUS reactivation in wild type or after treatments with 200 µM DHPA.

Supplemental Figure 5

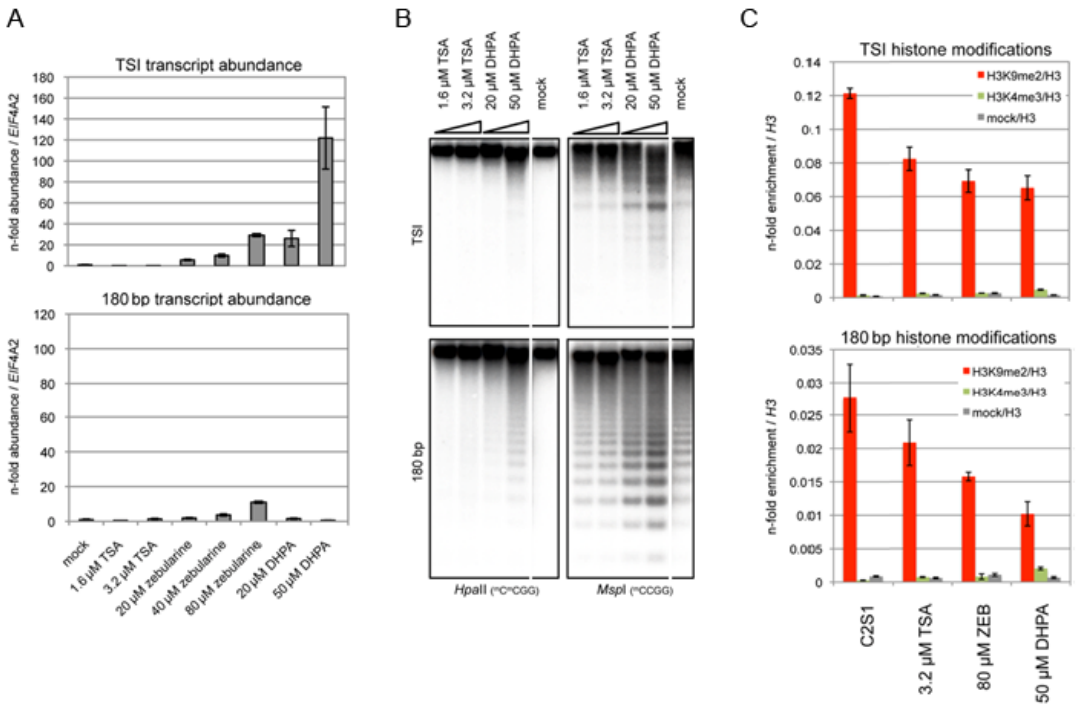

Supplemental Figure 5. Treatments with the SAHH inhibitor DHPA reduces levels of DNA and histone methylation at endogenous repeats.

(A) Quantification of repetitive TSI and 180bp read-through transcription in mock, TSA, zebularine and DHPA treated seedlings normalized to *EIF*4A2.

(B) DNA blot analysis for DNA methylation at TSI and 180bp repeats in mock, TSA, zebularine and DHPA treated seedlings.

(C) Quantitative measurements for H3K9me2 (red) and H3K4me3 (green) enrichment normalized to histone H3 at TSI and 180bp repeats and at *TUBULIN*8 as positive control. Grey columns represent samples precipitated without antibodies. Error bars in (A) and (C) represent standard deviation of triplicate analysis.

Supplemental Figure 6

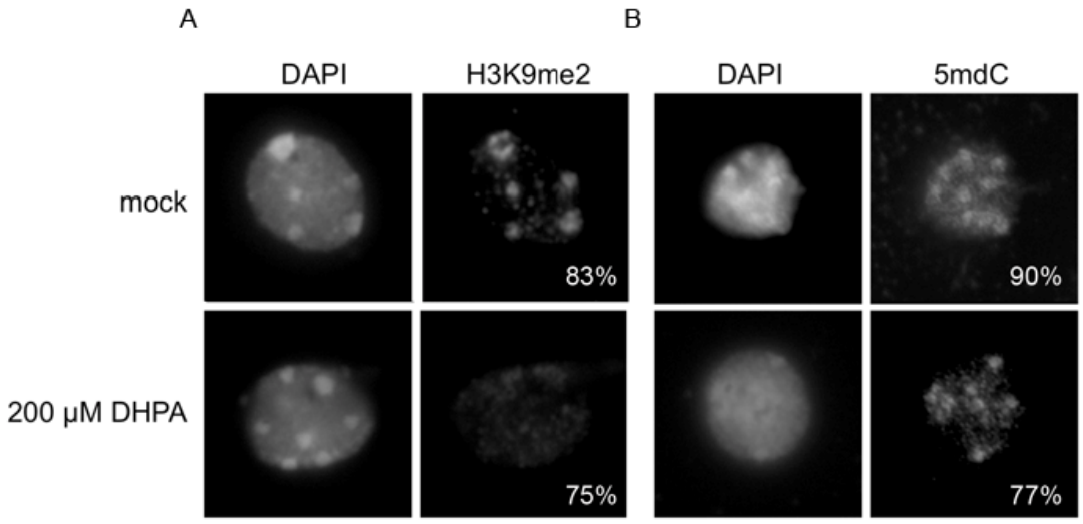

Supplemental Figure 6. DHPA treatment reduces H3K9me2, but not DNA methylation at chromocenters.

Cytological analysis of **(F)** H3K9me2 and **(G)** 5-methyldeoxycitosine after treatments with 200 µM DHPA. Percentage of nuclei with corresponding morphology is shown.

Supplemental Table 1

Sequence	analysis	target
AGTCTTTGGCTTTGTGTCTT	180bp probe	180bp repeats
TGGACTTTGGCTACACCATG		
AATTGAGATTTTTTAATAAAGGGTAATAT	bisulfite PCR	pCaMV35S1
ATCCCCCAAAATCCCCAAATA		
GTGATATCTCCACTGACGTAAGGG	qChIP	pCaMV35S1
ATATCTCATTGTCCCCCGGGA		
CCCATGGTGACCAAGAGTTT	qChIP, qPCR	LINE1-4
TCAATGTCGGAGACCTCCTC		
CTCTACCCTTTGCATTCATGAATCCTT	qChIP, qPCR	TSI
GATGGGCAAAAGCCCTCGGTTTTAAAATG		
ACCATCAAAGCTTTGAGAAGCAAGAAGAAGCTT	qChIP, qPCR	180bp repeats
CCATATGAGTCTTTGTCTTTGTATCTTCT		
GGGTAAATAGCTGCGCCGATGGTT	qPCR	HPT
CACGGCGGGAGATGCAATAGGTC		
ATCCAAGTTGGTGTGTTCTCC	qPCR	EIF4A2
GAGTGTCTCGAGCTTCCACTC		

Supplementary Table 1: DNA sequence of primers used throughout this study.